

1 Revised manuscript submitted to Chemosphere

2 2 September 2015

3

4 Colloidal mobilization of arsenic from mining-affected soils by
5 surface runoff

6

7

8 Miguel Angel Gomez-Gonzalez^a, Andreas Voegelin^b, Javier Garcia-Guinea ^a, Eduardo
9 Bolea ^c, Francisco Laborda ^c, Fernando Garrido^{a*}

10

11

12

13 ^a *Museo Nacional de Ciencias Naturales (MNCN, CSIC).C/ Jose Gutierrez Abascal 2,*
14 *28006, Madrid, Spain*

15 ^b *EAWAG, Swiss Federal Institute of Aquatic Science and Technology.*

16 *Ueberlandstrasse 133, 8600, Duebendorf, Switzerland*

17 ^c *Instituto Universitario de Ciencias Ambientales (IUCA), Universidad de Zaragoza. C/*
18 *Pedro Cerbuna 12, 50009, Zaragoza, Spain*

19

20

21 Keywords: Arsenic; runoff; colloids; AF4-ICP-MS; XAS; Rainfall simulation

22

23 *corresponding author. fernando.garrido@mncn.csic.es

ABSTRACT

Scorodite-rich wastes left as a legacy of mining and smelting operations pose a threat to environmental health. Colloids formed by the weathering of processing wastes may control the release of arsenic (As) into surface waters. At a former mine site in Madrid (Spain), we investigated the mobilization of colloidal As by surface runoff from weathered processing wastes and from sediments in the bed of a draining creek and a downstream sedimentation-pond. Colloids mobilized by surface runoff during simulated rain events were characterized for their composition, structure and mode of As uptake using asymmetric flow field-flow fractionation coupled to inductively plasma mass spectrometry (AF4-ICP-MS) and X-ray absorption spectroscopy (XAS) at the As and Fe K-edges. Colloidal scorodite mobilized in surface runoff from the waste pile is acting as a mobile As carrier. In surface runoff from the river bed and the sedimentation pond, ferrihydrite was identified as the dominant As-bearing colloidal phase. The results from this study suggest that mobilization of As-bearing colloids by surface runoff may play an important role in the dispersion of As from metallurgical wastes deposited above ground and needs to be considered in risk assessment.

1. INTRODUCTION

Mining and smelting operations have changed the global distribution and occurrence of metal(oid)s at the Earth's surface (Rauch, 2012), and the release of metals and metalloids from mining and processing wastes into aquatic and terrestrial environments may threaten environmental and human health. Human activities have led to substantial As contamination in the environment (Morin and Calas, 2006), as often occurs in association with economically relevant metal ores. Accordingly, the roasting and

smelting of metal ores has led to widespread environmental contamination via atmospheric emissions and deposition of waste materials (Vaughan, 2006). In Spain, there are many As-affected legacy sites affected from former mining activities. Often, As-bearing processing wastes had been dumped aboveground and remain exposed to rainfall and weathering, posing a risk for adjacent water bodies (Garcia-Sanchez and Alvarez-Ayuso, 2003).

The weathering of processing sulfide-containing wastes leads to the formation of acid mine drainage (AMD). The oxidation of Fe(II) and precipitation of Fe(III) in neutralized AMD may lead to the formation of mobile colloidal carriers for As (Cheng et al., 2009). Due to their physicochemical properties, colloids may persist in aqueous suspensions over extended periods of time and act as carriers for poorly soluble metals and metalloids in surface and subsurface environments (Kretzschmar and Sticher, 1997). The affinity of As to colloidal Fe(III) and the importance of such colloidal particles as As-mobilizing carriers in the environment has been documented (Fritzsche et al., 2011). For instance, Grosbois et al. (2011) identified different As-carriers during the transport of solid particulate matter in varying abundances according to the hydrological cycle of a river draining a former gold mine district in France. Furthermore, colloids and colloid-associated contaminants, mobilized by rainfall within ephemeral overland courses, can be transported rapidly through the vadose zone with minimal interaction with the soil matrix (Ranville et al., 2005). This can be attributed to the presence of preferential flow paths, which in turn may play a role in the solid-phase As distribution and As retention mechanism in soils, especially in locations affected by large amounts of metals released with AMD (Helmhart et al., 2012). Overall, the importance of surface runoff as compared to infiltration for As dispersion may vary with rainfall intensity and duration, vegetation cover, soil topography, as well as soil physical properties and flow

conditions through soils and riverbeds. Irrespective of the mode of colloid transport, the nature and stability of As-bearing colloids in tailings and mining wastes that control the extent of As release needs to be assessed.

The combined use of spectroscopic, spectrometric and fractionation techniques offers the means to gain information on the size-dependent elemental composition of colloids, the nature of the colloidal carrier phase, and the speciation of associated contaminants.

Rainfall simulation experiments on the other hand, allow to control rainfall parameters (intensity and duration) and to exclude the inherent variability associated with natural rain that increases the complexity of stormwater quality research (Bian et al., 2011). Simulated rainfall have been used to assess heavy metal contamination in urban areas (Wicke et al., 2012), but only few studies have been performed on contaminated soils under natural conditions (Fernandez-Galvez et al., 2008). To date, however, the colloid-facilitated release of As with surface runoff in mining-affected areas has not been assessed.

Asymmetric flow field-flow fractionation (AF4) is a separation technique for the characterization of colloids from natural samples (Laborda et al., 2011). When coupled to an inductively coupled plasma mass spectrometer (ICP-MS), the size-dependent elemental composition of the colloidal phases can be determined. For instance, Neubauer et al. (2013) characterized the colloid distribution in soil runoff as generated by storm events using AF4-ICP-MS. The authors showed that a colloidal fraction ranging from 0.2 to 0.45 μm was mobilized but they did not assess the speciation of the colloidal As. Direct insight into the speciation of colloidal As and Fe can be gained using X-ray absorption spectroscopy (XAS), widely used to study the speciation of As and Fe in natural samples (O'Day et al., 2004; Voegelin et al., 2007), including dispersible soil colloids (Regelink et al., 2014; Serrano et al., 2015).

In previous studies, we examined the dispersion and solid phase partitioning of As in soils and sediments affected by weathering and erosion of metallurgical processing wastes at a former mining and smelting site in Madrid province (Gomez-Gonzalez et al., 2014). In the same area, the molecular-scale speciation of As associated to colloids detached from soil extracts has previously been studied (Serrano et al., 2015). In this continuing work, we aimed at determining the extent and mode of colloidal As mobilization with surface runoff during simulated rain events. AF4-ICP-MS was used to determine the colloid size distribution and As partitioning between the dissolved and colloidal phase, and Fe and As K-edge XAS to determine the colloidal carrier phase and colloidal As speciation.

2. MATERIALS AND METHODS

2.1. Site description

The experiment was conducted in a sub-catchment of the Guadalix River (Madrid, Spain) at the foot of the ‘Sistema Central’ mountain range (40°45’34.33” N - 3°41’07.13” O, 929 meters altitude). In the area, metal sulfides and wolframite ores in association with quartz veins were mined for tungsten extraction during the Second World War. The abandoned smelting factory along with mining wastes deposited above ground still remain at this site (Helmhart et al., 2012). The massive pile of processing wastes (approximately 6x6 m, 1 meter-thick, 19 g As kg⁻¹), is subjected to weathering and erosion (Gomez-Gonzalez et al., 2014). The site is representative for many other legacy sites in Madrid province and other regions of Spain.

The average annual rainfall in the area reaches 705 mm and the average temperature, 13.3°C (Spanish Agency of Meteorology, AEMET). About 188-201 mm of the annual rain precipitate in winter, 197-213 mm in spring, 85-93 mm in summer and 200-233 in

autumn. Rainfall simulation tests were performed at: A) the arsenic-bearing waste pile (WP); B) the river bed (RB) of a small stream (~ 1 m wide) that seasonally collects surface runoff from WP; and C) the sediment that accumulates downstream in an artificial sedimentation pond (SP) (Figure S1). During intense rainfall, a major part of runoff waters is usually retained in the sedimentation pond remaining stagnant over several days until evaporation and infiltration lead to the drying out of the pond. Physical, chemical, and mineralogical properties of the topmost layer of soils and sediments at the experimental locations are in Table 1.

2.2. Rainfall simulation experiments

Simulation experiments were performed using the portable rainfall simulator designed by Calvo et al. (1988) and modified by Cerda et al. (1997). Single rainfall events of distilled water were applied at 28 mm h^{-1} during 60 minutes in each experimental location. The basic components of the simulator and the experimental conditions are described in the Supplementary Material (Figures S2 and S3).

2.3. Isolation of the colloid-suspensions in runoff

Three fractions of the runoff suspensions from the rainfall simulations were analyzed: (i) the colloid-containing suspension (CS, $\leq 1000 \text{ nm}$) obtained after centrifugation of the runoff suspension for the removal of particulate material, (ii) the solid colloids (1000-10 nm) isolated from the colloid-containing suspension by ultrafiltration using 10-nm membranes, and (iii) the dissolved fraction (DF) that passed 10-nm ultrafiltration membranes. The colloid-suspension (CS, $\leq 1000 \text{ nm}$) thus includes both the solid colloids (1000-10 nm) and the dissolved fraction ($\leq 10 \text{ nm}$). Runoff samples were subjected to the protocol described in the supplementary material (Figure S4).

2.4. Size characterization and elemental quantification by AF4-ICP-MS

The particle size distribution and elemental composition of the colloid suspensions were determined by AF4 (AF2000 model, *Postnova Analytics*) coupled to ICP-MS, a technique that has previously been shown to allow the determination of the size distribution of natural colloids generated in contaminated soils and the quantification of the colloidal mobilized metal(loid)s (Neubauer et al., 2013). An advantage of the AF4 technique is the mild separation conditions in absence of stationary phase, which preserves the original colloid size distribution. The AF4-ICP-MS specifications as well as recovery calculations are presented in the Supplementary Material (Tables S2 and S3).

2.5. As and Fe K-edge X-ray absorption spectroscopy (XAS) analyses

Arsenic and Fe XAS measurements were done on the colloids (1000-10 nm) isolated from the colloid suspension obtained from the waste-pile and the sedimentation-pond after 20 and 50 minutes of simulated rainfall. Arsenic and Fe K-edge EXAFS spectra were recorded at the bending magnet BM25A beamline at the ESRF-European Synchrotron Radiation Facility (Grenoble, France). Additional As EXAFS spectra from the SP colloids were recorded at beamline 22 of the ALBA Synchrotron Facility (Barcelona, Spain). Methods and reference materials are described in the Supplementary Material (Table S4).

3. RESULTS

3.1. Characterization of colloid-suspensions

The volumes, pH and electrical conductivity of runoff suspensions collected during the simulated 60-minutes rain events with 28 mm of rainfall are listed in Table 2. Given the

collected volumes and the total amount of distilled water applied per rain event, only 6% (WP) to 19% (RB) of the applied rainfall contributed to surface runoff, whereas the major fraction (94-81%) infiltrated into the subsurface. The acidity and electrical conductivity (EC) of the colloid-suspensions remained almost constant with time. The colloid concentration in the suspensions is summarized in Table 3 and Figure S5 (Supplementary Material). In the waste-pile and river-bed, with clay contents of 47% and 26% (Table 1), respectively, the colloid concentration in the suspensions remained almost constant with time over the rainfall simulation, while in the sedimentation-pond, with the lowest clay content (12%), the colloid concentration in the colloid-suspension decreased markedly during the initial 20 minutes of rainfall, and varied around a mean value of 0.26 mg L^{-1} over the rest of the irrigation period (Figure S5). The fractions of total As in runoff in colloidal form (97%, 0.8%, 22% for waste-pile, river-bed and sedimentation-pond, respectively) indicated near exclusive As mobilization in colloidal form from the waste-pile, an important colloidal As mobilization from the sedimentation-pond and only dissolved As mobilization from the river-bed (Table 3). The fraction of dissolved Fe was negligible in all cases, indicating near-exclusive association of Fe with suspended colloids. The molar As/Fe ratio in colloids immobilized from the waste-pile zone was near unity, while this parameter was 0.36-0.58 and 0.05 in colloids from river-bed and sedimentation-pond, respectively. This disparity pointed to differences in the As mode of association to colloids that warrant examination by XAS. Both As and Fe concentrations in the colloid-suspension expressed per mass of colloids decreased at the end of the experiments (50 minutes), although the colloid concentration itself remained constant. Notably, the As concentration in the colloidal phase was about 1.9 (river-bed) to 2.9 (waste-pile and sedimentation-pond) times higher

than in the corresponding bulk materials (Tables 1 and 3), indicating that As was enriched in the colloid-size fraction of the waste and sediment materials. Conversely, the Fe concentration in colloids mobilized from the waste-pile was similar to the Fe concentration in the waste material, whereas the Fe concentration in colloids mobilized from the river-bed and the sedimentation-pond decreased 5-10 times. This could be partially explained by the formation of Fe-(hydr)oxide coatings (Gomez-Gonzalez et al., 2014) on the surface of aluminum-silicate particles (Table 1) larger than the size of colloids (< 1000 nm) in both the river-bed and the sedimentation-pond.

3.2. Size characterization of the colloids from the sedimentation-pond

The colloid suspensions from the waste-pile and the river-bed could not be measured by AF4. In the waste-pile this was due to the high electrical conductivity of its runoff suspensions (Table 2) which led to irreversible colloids absorption onto the AF4 channel membrane. The colloid concentrations in the runoff suspensions from the river-bed were too low to be determined by AF4 (Table 3, Figure S6). Conversely, the particle size distribution and associated As, Fe and Al concentrations in the colloid-suspensions (20, 35 and 50 minutes) of the sedimentation-pond zone were obtained by AF4-ICP-MS (Figures 1 and S7). Size distribution maxima were 147 nm, 160 nm and 195 nm for the colloid-suspensions obtained at 20, 35 and 50 minutes of rainfall, respectively. The maxima corresponding to the secondary shoulder visible at 20 and 35 minutes and to the defined secondary peak at 50 minutes of rainfall varied little (~ 460 nm) as estimated by fitting the fractograms to a double-peak lorentzian function (Figure 1a). Concentration maxima were estimated by fitting a lognormal function (Figure 1b; maxima, white circle; confidence interval (colour line) at 95% probability). Arsenic and

Fe concentration maxima appeared at 143, 115 and 136 nm for the colloid-suspension obtained at 20, 35 and 50 minutes of irrigation time, indicating a similar behavior of these elements in the colloidal mobilization. The Al concentration maxima appeared at 156, 121 and 166 nm for the same irrigation times.

3.3. Speciation of colloidal As and Fe by K-edge XAS

The As and Fe K-edge XANES spectra of colloids isolated from runoff from the waste-pile and sedimentation-pond (Figure S8, Supplementary Material), indicated As(V) and Fe(III) as the dominant oxidation states. The As and Fe K-edge EXAFS spectra of colloids from the waste-pile runoff and XANES spectra of colloids from the sedimentation-pond together with the reconstructed linear combination fitting (LCF) spectra are shown in Figure 2 and the LCF results are listed in Table 4. In the case of colloids from the sedimentation-pond, only the XANES spectra were evaluated due to the low quality of the corresponding EXAFS spectra. Arsenic K-edge EXAFS spectra from the waste-pile runoff indicated a major contribution (91–94%) from scorodite and minor contribution of As(V) sorbed to ferrihydrite (6–9%) at both irrigation times. Iron K-edge EXAFS spectra also showed a major contribution from scorodite (91–96%) and minor amounts of nontronite (9%) and hematite (4%). Results from shell-by-shell fit analysis of As and Fe K-edge EXAFS spectra of colloids from the waste-pile were in line with a dominant fraction of As and Fe in scorodite (Table S5, details on shell-fit procedure in Supplementary Material).

The LCF analysis of the As and Fe K-edge XANES spectra of colloids from the sedimentation-pond on the other hand, revealed a dominant fraction of As(V) sorbed to ferrihydrite and Fe(III) in smectite (50%), nontronite (21–27%) and schwertmannite

(23–29%) (Table 4, Figure 2) suggesting that Fe was mainly contained in clay minerals, and to a lesser extent poorly crystalline Fe(III)-(hydr)oxides.

4. DISCUSSION

4.1. Colloidal scorodite as potential nanovector for As dispersion with surface runoff

Although scorodite may be thermodynamically unstable when exposed to water containing low Fe and As concentrations, the dissolution of synthetic scorodite over the pH range 5-9 has been shown to be slow (Bluteau and Demopoulos, 2007), and Paktunc and Bruggeman (2010) reported that As solubility in equilibrium with scorodite is lowest at pH 3-4. Our results show that colloidal scorodite mobilized with surface runoff is acting as a mobile As carrier. Molecular-scale colloidal As speciation confirms the presence of scorodite in the colloids isolated from the waste-pile colloid-suspensions (Tables 4 and S5, Figure 2). These results are in agreement with the molar As/Fe ratio in the colloid-suspension (Table 3) and the XRD analyses (Table 1). The colloidal stability and mobility of scorodite is expected to depend on its surface charge, but respective data is scarce. According to Robins (1987), scorodite formed at pH < 1.8 exhibit a negative surface charge, whereas the formation of a surface Fe(III)-(hydr)oxide may lead to a positive surface charge. Other surface transformation on the colloidal scorodite may also take place affecting the stability of weathered scorodite colloids.

From the waste-pile material, As was mainly mobilized in colloidal form, with colloidal As concentrations between 3512 and 4488 $\mu\text{g L}^{-1}$. Based on the average As concentration in the colloid-suspensions from the waste-pile (Table 3) and the volume of surface runoff, about 6.7 mg of colloidal As were released with the surface runoff from the irrigated area (0.24 m²) during the 60-minutes rainfall simulation, corresponding to

~28mg colloidal As per m²waste-pile surface. Considering that the dumped processing wastes cover about 36 m², roughly 1 g of colloidal As could be released by surface runoff during a natural rainfall event with a duration and intensity similar to the simulation (60 minutes, 28 mm of rainfall). During the simulated rainfall event, 6% of the water volume applied to the waste pile surface was collected as surface runoff (Table 2), suggesting that most water infiltrated into the waste material. Colloidal scorodite could also contribute to vertical transport of As into deeper soil horizons. Indeed, a recent study at the same site (Gomez-Gonzalez et al., 2014) indicated the presence of scorodite at greater depths, although the fraction of scorodite decreased with depth at the expense of As(V) sorbed to Fe(III)-(hydr)oxides. Rainfall intensity and duration affect the runoff/infiltration ratio and this should be considered site-specific. In the studied area, rainfall events with > 10 mm occur on average on 18.5 days per year, and storm events with > 30 mm of precipitation on 2 days per year (Guía resumida del clima en España (1981-2010), www.aemet.es). This indicates that the potential for continuing As dispersion via colloidal As release and surface runoff is substantial unless remediation actions are taken.

4.2. Potential migration of colloidal As into the downstream soils

Arsenic-bearing colloids in runoff suspensions from the river-bed and the sedimentation-pond greatly differ from those identified in the waste-pile zone. Two processes are depicted from our results: First, virtually no colloidal scorodite mobilized from the waste-pile appears at the river-bed. At this second experimental zone, colloidal As concentrations are negligible compared to dissolved ones (Table 3). Along the river-bed, a large fraction of As released after scorodite dissolution might be leached through the river-bed itself, and through preferential flow paths in the subsoil, as suggested by

Helmhart et al.(2012). Second, in the sedimentation-pond, where a major part of runoff waters is retained and may remain stagnant over several days before drying out, colloidal As is mostly As(V) associated with ferrihydrite or other Fe(III)-(hydr)oxides. The increasing pH in the river-bed and sedimentation-pond, i.e., with increasing distance from the waste pile may favor scorodite dissolution and As(V) resorption to (amorphous) Fe(III)-(hydr)oxide colloids(Serrano et al., 2015).Ferrihydrite has a high capacity for As(V) uptake(Fritzsche et al., 2011), and their association has been extensively reported(Johnson and Hallberg, 2005). The present study indicates that a fraction of As-bearing Fe(III)-(hydr)oxide colloids contained in the sedimentation-pond as spectroscopically described in the dispersible colloidal fraction by Serrano et al. (2015) are potentially mobilizable and may behave as colloidalAs carriers within runoff generated by strong rain events. The differences in colloid size-distributions derived from AF4-UV-vis (Figure 1a) and AF4-ICP-MS fractograms (Figure 1b) as well as the slight discrepancy in temporal trends of Fe and Al (Figures 1b and S7) may be due to Al-containing clay minerals in the colloidal fraction of the sedimentation-pond runoff (Table 4), whose laminar structure affects the hydrodynamic diameter of the particles measured by AF4. The use of distilled water as rainfall instead of artificial rainwater with background electrolyte concentrations may introduce some disparity with natural rain events. However,Vazquez et al. (2003)reported ionic rainfall compositions in NW Spain with a range of electrical conductivities similar to the ones obtained in our river-bed and sedimentation-pond runoff suspensions. According to that, we would not expect drastic differences in the use of distilled water rather than a slight enhance of colloids release.

5. CONCLUSIONS

The results from this study suggest that colloidal scorodite may be released from mining wastes and act as an As carrier in surface runoff. Similarly, As(V) immobilize by sorption to Fe(III)-(hydr)oxides in the sediments from the sedimentation-pond may be susceptible to mobilization in colloidal form.

Deposited mine wastes from legacy mining activities in Spain, should therefore be isolated to reduce weathering and colloid transport with surface runoff which may result in the dispersion of As in both colloidal and dissolved As form. This should be taken into account when As-rich metallurgical wastes are deposited above ground, because both scorodite and ferrihydrite should not be considered as effective trapping systems of As(V). More research is needed, however, to better quantify the importance of As mobilization with surface and subsurface runoff in colloidal and dissolved form in order to effectively prevent As release to the environment. Also, the application of any capping system aiming to prevent the wastes from erosion could limit the colloids and contaminants migration in the environment.

Rainfall simulation experiments and advanced separation techniques such as AF4-ICP-MS are suitable analytical procedures to characterize suspended colloids in runoff and study their potential for colloid-facilitated contaminant release and transport. XAS provides complementary molecular-level insight into the speciation of inorganic contaminants in the colloidal phase.

ACKNOWLEDGEMENTS

The Spanish Ministry of Economy and Competitiveness (research project CGL2010-17434) supported this study. M.A. Gomez-Gonzalez was supported by the Ph.D. Spanish FPI fellowship (BES-2011-046461) and by graduate students (EEBB-I-14-08063) programs. XAS measurements on BM25A beamline (ESRF) were supported by

the project EV-41; XAS measurements on BL22–CLAESS beamline (ALBA-CELLS) were supported by the project 2012100332. ICP-OES and ICP-MS analyses were performed at *Servicio de análisis químico (Servicio General de Apoyo a la Investigación-SAI), Universidad de Zaragoza*.

FIGURE CAPTIONS

1– (a) AF4-UV-vis fractograms of colloid-suspension from the sedimentation-pond at 20 (black), 35 (red), and 50 minutes (blue). (b) Concentration maxima (white circle) fractograms and confidence interval (colour line) at 95% probability. Dotted line represents the average size maxima of all elements and times (131 nm of size).

2– Arsenic (a) and iron (b) K-edge EXAFS spectra of waste-pile (WP) colloids. Arsenic (c) and iron (d) XANES spectra of sedimentation-pond (SP) colloids. Black lines, experimental data; red lines, LCF results (Table 4 for LCF values).

REFERENCES

- Bian B, Cheng X-J, Li L. Investigation of urban water quality using simulated rainfall in a medium size city of China. *Environmental Monitoring and Assessment* 2011; 183: 217-229.
- Bluteau MC, Demopoulos GP. The incongruent dissolution of scorodite - Solubility, kinetics and mechanism. *Hydrometallurgy* 2007; 87: 163-177.
- Calvo A, Gisbert J, Palau E, Romero M. Un simulador de lluvia portatil de facil construccion. Eds. M. Sala and F. Gallart. *Metodos y Tecnicas para la medicion de procesos geomorfologicos* 1988; SEG Monogr.: 6-15, Spain.
- Cerda A, Ibanez S, Calvo A. Design and operation of a small and portable rainfall simulator for rugged terrain. *Soil Technology* 1997; 11: 163-170.

374 Cornell RM, Schwertmann U. The Iron Oxides: Structure, Properties, Reactions,
 375 Occurrences and Uses. Wiley-VCH Verlag GmbH & Co. KGaA, 2004.
 376 Cheng H, Hu Y, Luo J, Xu B, Zhao J. Geochemical processes controlling fate and
 377 transport of arsenic in acid mine drainage (AMD) and natural systems. Journal
 378 of Hazardous Materials 2009; 165: 13-26.
 379 Fernandez-Galvez J, Barahona E, Mingorance MD. Measurement of infiltration in small
 380 field plots by a portable rainfall simulator: Application to trace-element
 381 mobility. Water Air and Soil Pollution 2008; 191: 257-264.
 382 Fritzsche A, Rennert T, Totsche KU. Arsenic strongly associates with ferrihydrite
 383 colloids formed in a soil effluent. Environmental Pollution 2011; 159: 1398-
 384 1405.
 385 Garcia-Sanchez A, Alvarez-Ayuso E. Arsenic in soils and waters and its relation to
 386 geology and mining activities (Salamanca Province, Spain). Journal of
 387 Geochemical Exploration 2003; 80: 69-79.
 388 Gomez-Gonzalez MA, Serrano S, Laborda F, Garrido F. Spread and partitioning of
 389 arsenic in soils from a mine waste site in Madrid province (Spain). Science of
 390 the Total Environment 2014; 500–501: 23-33.
 391 Grosbois C, Courtin-Nomade A, Robin E, Bril H, Tamura N, Schäfer J, et al. Fate of
 392 arsenic-bearing phases during the suspended transport in a gold mining district
 393 (Isle river Basin, France). Science of the Total Environment 2011; 409: 4986-
 394 4999.
 395 Helmhart M, O'Day PA, Garcia-Guinea J, Serrano S, Garrido F. Arsenic, Copper, and
 396 Zinc Leaching through Preferential Flow in Mining-Impacted Soils. Soil Science
 397 Society of America Journal 2012; 76: 449-462.

398 Johnson DB, Hallberg KB. Acid mine drainage remediation options: a review. Science
399 of the Total Environment 2005; 338: 3-14.

400 Kretzschmar R, Sticher H. Transport of Humic-Coated Iron Oxide Colloids in a Sandy
401 Soil: Influence of Ca²⁺ and Trace Metals. Environmental Science &
402 Technology 1997; 31: 3497-3504.

403 Laborda F, Ruiz-Begueria S, Bolea E, Castillo JR. Study of the size-based
404 environmental availability of metals associated to natural organic matter by
405 stable isotope exchange and quadrupole inductively coupled plasma mass
406 spectrometry coupled to asymmetrical flow field flow fractionation. Journal of
407 Chromatography A 2011; 1218: 4199-4205.

408 Morin G, Calas G. Arsenic in soils, mine tailings, and former industrial sites. Elements
409 2006; 2: 97-101.

410 Neubauer E, von der Kammer F, Knorr KH, Peiffer S, Reichert M, Hofmann T.
411 Colloid-associated export of arsenic in stream water during stormflow events.
412 Chemical Geology 2013; 352: 81-91.

413 O'Day PA, Rivera N, Root R, Carroll SA. X-ray absorption spectroscopic study of Fe
414 reference compounds for the analysis of natural sediments. American
415 Mineralogist 2004; 89: 572-585.

416 Paktunc D, Bruggeman K. Solubility of nanocrystalline scorodite and amorphous ferric
417 arsenate: Implications for stabilization of arsenic in mine wastes. Applied
418 Geochemistry 2010; 25: 674-683.

419 Ranville JF, Chittleborough DJ, Beckett R. Particle-size and element distributions of
420 soil colloids: Implications for colloid transport. Soil Science Society of America
421 Journal 2005; 69: 1173-1184.

- Rauch JN. The present understanding of Earth's global anthrobiogeochemical metal cycles. *Mineral Economics* 2012; 25: 7-15.
- Regelink IC, Voegelin A, Weng L, Koopmans GF, Comans RNJ. Characterization of Colloidal Fe from Soils Using Field-Flow Fractionation and Fe K-Edge X-ray Absorption Spectroscopy. *Environmental Science & Technology* 2014; 48: 4307-4316.
- Robins RG. Solubility and Stability of Scorodite, $\text{FeAsO}_4 \cdot 2\text{H}_2\text{O}$ - Discussion. *American Mineralogist* 1987; 72: 842-844.
- Serrano S, Gomez-Gonzalez MA, O'Day PA, Laborda F, Bolea E, Garrido F. Arsenic speciation in the dispersible colloidal fraction of soils from a mine-impacted creek. *Journal of Hazardous Materials* 2015; 286: 30-40.
- Vaughan DJ. Arsenic. *Elements* 2006; 2: 71-75.
- Vazquez A, Costoya M, Pena RM, Garcia S, Herrero C. A rainwater quality monitoring network: a preliminary study of the composition of rainwater in Galicia (NW Spain). *Chemosphere* 2003; 51: 375-386.
- Voegelin A, Weber FA, Kretzschmar R. Distribution and speciation of arsenic around roots in a contaminated riparian floodplain soil: Micro-XRF element mapping and EXAFS spectroscopy. *Geochimica Et Cosmochimica Acta* 2007; 71: 5804-5820.
- Wicke D, Cochrane TA, O'Sullivan AD. Atmospheric deposition and storm induced runoff of heavy metals from different impermeable urban surfaces. *Journal of Environmental Monitoring* 2012; 14: 209-216.

Table 1 – Physical and chemical properties of bulk samples

Characteristics	Samples		
	WP	RB	SP
<i>pH</i> ^a	3.3	4.3	6.1
<i>E.C. (μS cm⁻¹)</i> ^b	2320	93.7	110
<i>ECEC (eq kg⁻¹)</i> ^c	0.79	0.11	0.05
<i>TOC (%)</i> ^d	0.03	0.24	0.20
<u>Soil texture (%)</u> ^e			
<i>Sand</i>	53	30	70
<i>Silt</i>	-	44	18
<i>Clay</i>	47	26	12
<u>Element concentration (mg kg⁻¹)</u> ^f			
<i>Al</i>	1100	422	257
<i>Fe</i>	25230	45530	16980
<i>Cu</i>	1390	99	52
<i>Zn</i>	151	82	73
<i>As</i>	14390	620	94
<i>Pb</i>	465	29	22
<u>Mineralogical composition</u> ^g			
<i>Major phases</i>	Scorodite Gypsum	Illite Kaolinite Quartz	Illite Microcline Kaolinite Albite
<i>Minor phases</i>	Quartz Hematite	Muscovite Albite	Quartz Montmorillonite

^aPotassium chloride (KCl, 3 mol L⁻¹) was used as electrolyte solution for pH measurements
^bE.C. = Electrical conductivity
^cECEC = Effective Cation exchange capacity as the sum of Ca, Mg, Na, K and Al (Shuman 1990)
^dTOC = Total organic carbon determined by wet digestion (Walkley and Black 1934)
^eTexture was determine by the pipette method after removing soil organic matter (Gee and Bauder 1982)
^fPseudo-total concentration measured by ICP-OES after aqua regia + microwave digestion (Chen and Ma 2001)
^gDetermined by qualitative XRD analysis. Major phases are those with more than 15 % contribution to the total composition

Table 2 – Physical characteristics of the collected runoff suspensions^a

Sampling location	Runoff time	Runoff volume ^b	<i>pH</i>	Electrical Conductivity
	<i>min</i>	<i>mm</i>		<i>μS cm⁻¹</i>
WP	0-10	0.27	3.90	1567
	10-20	0.23	4.08	1532
	20-30	0.27	4.16	1580
	30-40	0.24	4.04	1640
	40-50	0.30	4.14	1585
	50-60	0.32	4.20	1548
	Total surface runoff ^c	1.63 (6%)		
RB	0-5	0.45	4.54	198
	5-10	0.45	4.60	164
	10-15	0.47	4.63	143
	15-20	0.45	4.64	133
	20-25	0.44	4.60	147
	25-30	0.43	4.52	163
	30-35	0.37	4.57	169
	35-40	0.40	4.63	160

	40-45	0.46	4.56	159
	45-50	0.44	4.54	156
	50-55	0.48	4.68	136
	55-60	0.49	4.54	157
	<i>Total surface runoff^c</i>	5.33 (19 %)		
SP	0-5	0.28	6.24	53
	5-10	0.31	6.26	52
	10-15	0.30	6.44	44
	15-20	0.37	6.33	43
	20-25	0.39	6.41	40
	25-30	0.42	6.18	41
	30-35	0.44	5.96	46
	35-40	0.46	5.90	38
	40-45	0.48	5.94	37
	45-50	0.45	6.25	33
	50-55	0.44	6.34	30
	55-60	0.48	6.43	23
	<i>Total surface runoff^c</i>	4.81 (17 %)		

^aDistilled water was used in the rainfall simulation tests

^bVolume of runoff collected during the rainfall simulation test at waste-pile (WP), river-bed (RB) and sedimentation-pond (SP)

^cDefined as the sum of all volumes collected during the experiment. The percentage of water collected respect to the total water pumped during the experiment (28 mm) is presented in parenthesis

Table 3 –As and Fe concentrations of colloid (≤ 1000 nm) suspensions (CS) and dissolved fractions (DF) ≤ 10 nm (\pm standard deviation, $n=3$ ^a)

Sample	Time	Fraction	As	Fe	Colloid concent. ^d	Molar As/Fe ratio	As concent.	Fe concent.
			$\mu\text{g L}^{-1}$ ^{b,c}		mg L^{-1}		$\text{mg kg colloid}^{-1}$ ^e	
WP	20 min	CS	4500 \pm 5	3230 \pm 303				
		DF	128 \pm 7	< QL	109	1.04	41 \cdot 10 ³	30 \cdot 10 ³
		Colloids	4372 ^f	3230				
WP	40 min	CS	4600 \pm 23	3480 \pm 215				
		DF	112 \pm 2	< QL	95	0.98	48 \cdot 10 ³	36 \cdot 10 ³
		Colloids	4488	3480				
WP	50 min	CS	3590 \pm 18	2660 \pm 382				
		DF	78 \pm 2	< QL	102	1.01	35 \cdot 10 ³	26 \cdot 10 ³
		Colloids	3512	2660				
RB	20 min	CS	281 \pm 6	588 \pm 303				
		DF	298 \pm 4	< QL	200	0.36	1410	2940
		Colloids	-	588				
RB	35 min	CS	262 \pm 6	587 \pm 185				
		DF	260 \pm 6	< QL	207	0.33	1270	2840
		Colloids	2	587				
RB	50 min	CS	146 \pm 7	186 \pm 206				
		DF	148 \pm 8	< QL	154	0.58	950	1210
		Colloids	-	186				
SP	20 min	CS	131 \pm 5	1870 \pm 253				
		DF	100 \pm 4	< QL	399	0.05	330	4690
		Colloids	31	1870				
SP	35 min	CS	128 \pm 6	1990 \pm 290				
		DF	106 \pm 5	< QL	437	0.05	290	4550
		Colloids	22	1990				
SP	50 min	CS	96 \pm 6	1060 \pm 348				
		DF	72 \pm 6	< QL	427	0.05	200	2200
		Colloids	24	1060				

^aStandard deviation was calculated by triplicate determination of the same aliquot

^bElemental concentration was expressed on μg of metal per liter of colloid suspension (CS)

^cQuantification limits (QL) for ICP-MS measurement of As was $0.1 \mu\text{g L}^{-1}$ and $73 \mu\text{g L}^{-1}$ for ICP-OES measurements of Fe

^dMass of colloids calculated according to Plathe et al. 2010

^eMilligrams of As and Fe per kilogram of colloids (1000-10 nm)

^fAs and Fe concentrations of colloids (1000-10 nm) were defined as the difference between the concentration of the CS and the DF

Table 4 – Linear combination fit results for As and Fe K-edge EXAFS or XANES spectra

<i>As EXAFS / XANES</i> ^a												
Sample	Scorodite ^b		As sorbed to Ferrihydrite ^b		R Factor ^e	red χ^2 ^f						
	% ^c	ΔeV ^d	%	ΔeV								
WP												
20 min ^g	94.2	-	5.7	-	0.0249	0.8562						
WP												
50 min ^g	91.3	-	8.7	-	0.0199	0.6527						
SP												
20 min ^h			99.7	- 0.3	0.0116	0.0062						
SP												
50 min ^h			99.6	- 0.4	0.0125	0.0068						
<i>Fe EXAFS / XANES</i> ^a												
Sample	Scorodite ^b		Nontronite ^b		Hematite ^b		Smectite ^b		Schwertmannite ^b		R factor	red χ^2
	%	ΔeV	%	ΔeV	%	ΔeV	%	ΔeV	%	ΔeV		
WP												
20 min ⁱ	91.1	-	8.6	-							0.0517	0.665
WP												
50 min ⁱ	95.7	-			4.2	-					0.0505	0.619
SP												
20 min ^j			27.1	0.1			50.3	- 0.1	23.3	0.2	0.0003	0.0001
SP												
50 min ^j			20.9	0.3			50.4	- 0.1	29.3	- 0.1	0.0003	0.0001

^aEXAFS spectra of waste-pile(WP) colloids and XANES spectra of sedimentation-pond (SP) colloids were analyzed by LCF analyses

^bThe scorodite reference spectrum was obtained from Savage et al. (2005). The As(V) sorbed to ferrihydrite spectrum was obtained from Root et al. (2009). The nontronite (NAu-1) spectrum was obtained from Gorski et al. (2013). The hematite and smectite spectra were obtained from O'Day et al. (2004). The schwertmannite spectrum was measured by S. Hayes in the BM 4-1(SSRL, Stanford, USA, unpublished) (Table S4, Supplementary Material)

^cFittings were not constrained to sum 100 %

^dFitting variations of XANES LCF given by the software Athena (Ravel and Newville 2005)

^eNormalized sum of the squared residuals of the fit [$R = \sum(\text{data-fit})^2 / \sum \text{data}^2$]

^fGoodness-of-fit was assessed by the χ^2 statistic [$= (\text{F factor}) / (\text{no. of points} - \text{no. of variables})$]

^gLCF EXAFS range: 2 – 11 Å, spectra measured at ESRF (Grenoble, France)

^hLCF XANES range: 11855 – 11935 eV, spectra measured at ALBA (Barcelona, Spain)

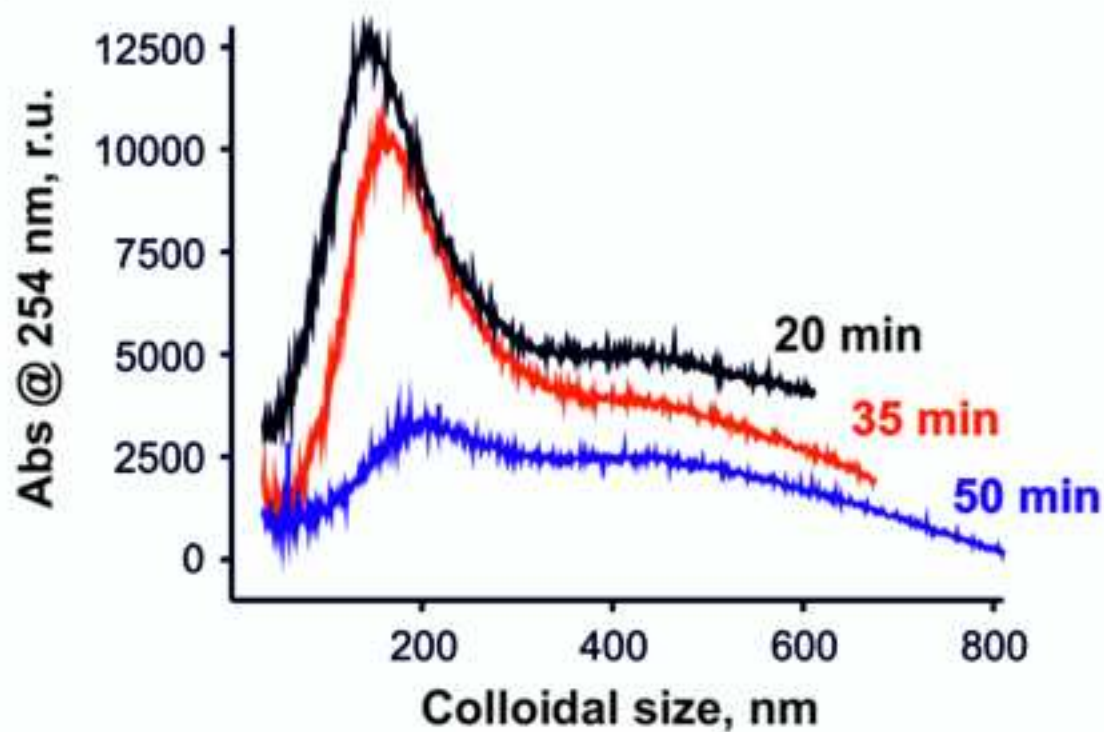
ⁱLCF EXAFS range: 2 – 9 Å, spectra measured at ESRF (Grenoble, France)

^jLCF XANES range: 7105 – 7185 eV, spectra measured at ESRF (Grenoble, France)

Figure

[Click here to download high resolution image](#)

a



b

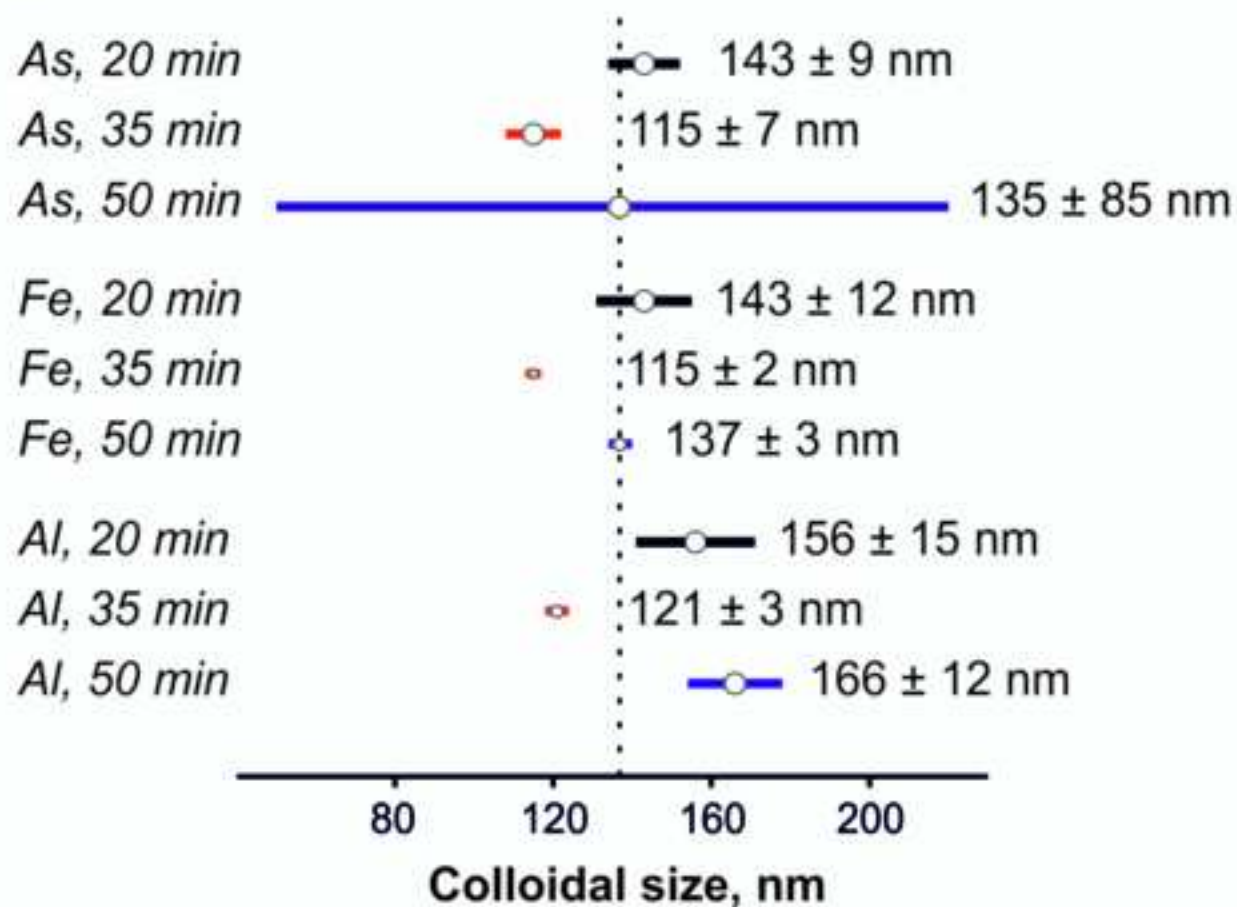
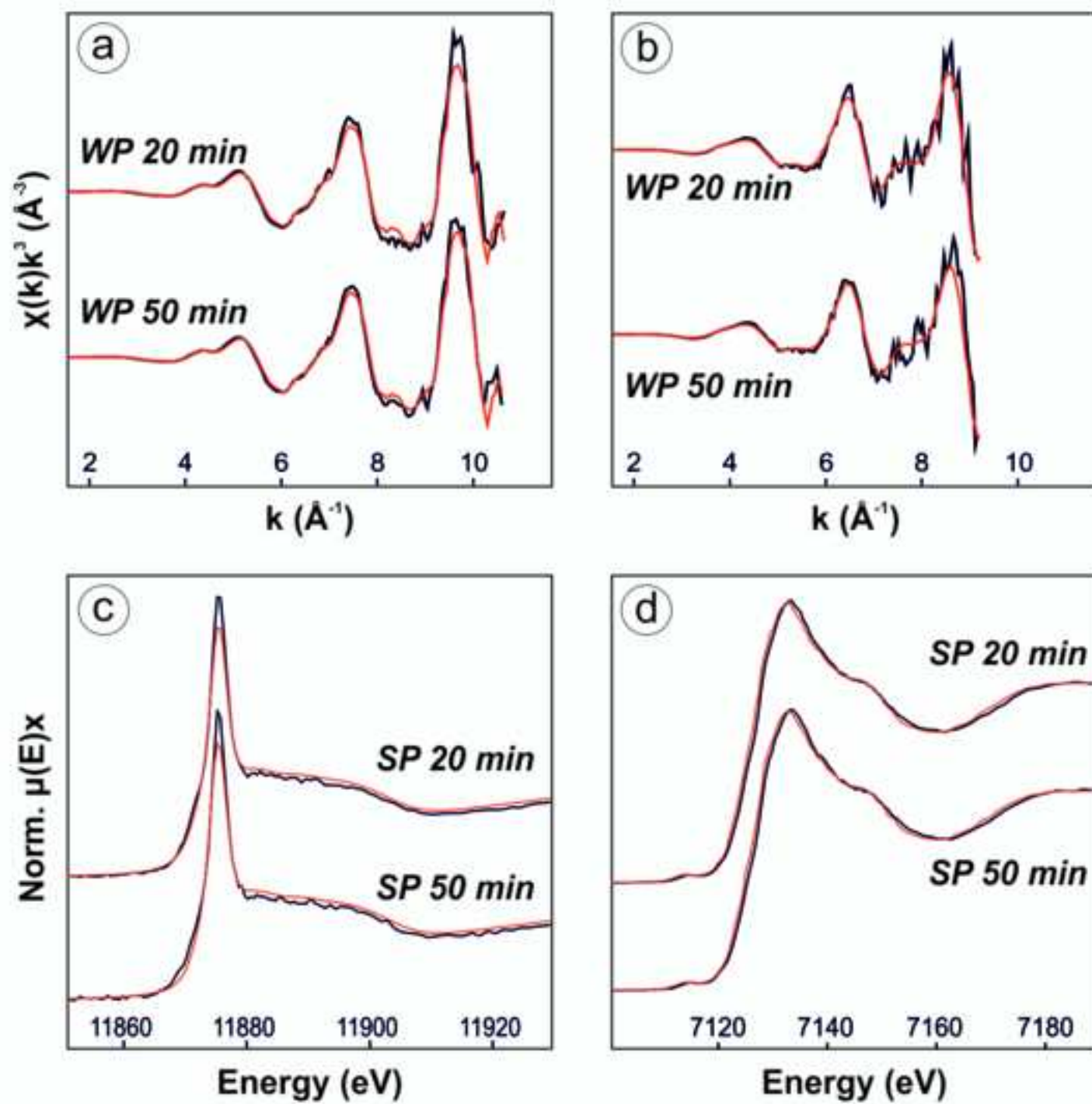


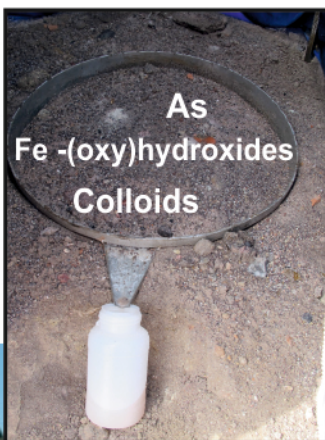
Figure 2
[Click here to download high resolution image](#)



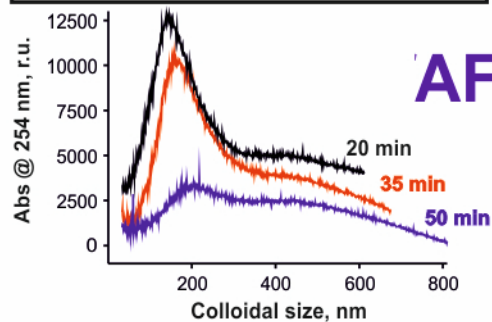
Supplementary Material

[Click here to download Supplementary Material: Rainfall Simulation_SM_Revised.pdf](#)

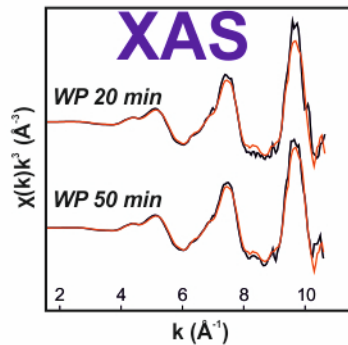
Graphical Abstract



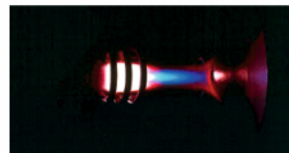
[Colloid suspension]^{<1000nm}



[Colloids]^{1000-10nm}



[Dissolved]^{<10nm}



ICP-MS